Biochemical and Biophysical Research Communications 444 (2014) 662–669

Contents lists available at ScienceDirect

Biochemical and Biophysical Research Communications

journal homepage: www.elsevier.com/locate/ybbrc

Sirt3 controls chromosome alignment by regulating spindle dynamics during mitosis

Byung-Soo Choi, Ji Eun Park, Chang-Young Jang *

Research Center for Cell Fate Control, College of Pharmacy, Sookmyung Women's University, Seoul 140-742, Republic of Korea

ARTICLE INFO

Article history:
Received 21 January 2014
Available online 1 February 2014

Keywords:
Sirt3
Spindle assembly checkpoint
Chromosome alignment
Spindle dynamics

ABSTRACT

Sirt3, one of mammalian sirtuins is a prominent mitochondrial deacetylase that controls mitochondrial oxidative pathways and the rate of reactive oxygen species. Sirt3 also regulates energy metabolism by deacetylating enzymes involved in the metabolic pathway related with lifespan. We report here a novel function of Sirt3 which was found to be involved in mitosis. Depletion of the Sirt3 protein generated unaligned chromosomes in metaphase which caused mitotic arrest by activating spindle assembly checkpoint (SAC). Furthermore, the shape and the amount of the spindles in Sirt3 depleted cells were abnormal. Microtubule (MT) polymerization also increased in Sirt3 depleted cells, suggesting that Sirt3 is involved in spindle dynamics. However, the level of acetylated tubulin was not increased significantly in Sirt3 depleted cells. The findings collectively suggest that Sirt3 is not a tubulin deacetylase but regulates the attachment of spindle MTs to the kinetochore and the subsequent chromosome alignment by increasing spindle dynamics.

1. Introduction

Sirtuins consist of seven deacetylase family (Sirt1–Sirt7) which has NAD^+-dependent protein deacetylase and/or ADP-ribosyltransferase activities [1]. Mammalian sirtuins have been identified as homologs of SIR2 (silent information regulator 2), a histone deacetylase involved not only in the positive effects of caloric restriction on the longevity of lifespan but in gene expression by chromatin silencing [2]. Whereas histone deacetylase removes an acetyl group from histone, sirtuins deacetylates a variety of proteins including transcription factors and metabolic enzymes [3]. Therefore, sirtuins are crucial factors responsible for metabolic and oxidative stress and are related to diseases associated with aging [4]. It has been reported that Sirt1, Sirt6, and Sirt7 mainly localize in the nucleus, Sirt2 is in the cytoplasm, and Sirt4 and Sirt5 in the mitochondria. Sirt3 primarily localizes in the mitochondria but translocates from the nucleus to the mitochondria under cellular stress conditions [5].

Individual sirtuins have specific substrates in different metabolic or signaling pathways. Sirt1 deacetylates lysine 9 in histone H3 (H3K9), lysine16 in histone H4 (H4K16), and nonhistone proteins involved in metabolism, cell growth, apoptosis, adaptation to caloric restriction, and tumorigenesis [6,7]. Sirt2 is a histone deacetylase and controls acetylation of histone H4 lysine 16 (H4K16Ac) [8]. Sirt3, a mitochondrial deacetylase, controls global mitochondrial lysine acetylation and acts as a tumor suppressor by maintaining mitochondrial integrity and metabolism [9]. Sirt4 negatively regulates glutamate dehydrogenase and decreases the effect of calorie restriction in some cell types [10,11]. Sirt5 controls the urea cycle by deacetylating carbamoyl phosphate synthetase 1 [12] and also has a protein lysine desuccinylase activity and a protein lysine demalonylase activity [13]. Sirt6 is also histone deacetylase and acts as a tumor suppressor by controlling cancer metabolism [14]. Sirt7 regulates the transcription of rRNA genes by interacting with RNA polymerase I [15]. Several sirtuins such as Sirt1 and Sirt2 are involved in the mitotic process. Sirt1 is associated with chromosome instability in mitosis [16]. Sirt2 has tubulin deacetylase activity in addition to histone deacetylase activity and regulates chromosome condensation and spindle dynamics [17]. During mitosis, Sirt2 interacts with various mitotic structures such as centrosome, mitotic spindle, and midbody in order to maintain genome integrity.

Progression of mitosis consists of dynamic processes such as nuclear envelop breakdown, centrosome maturation, spindle nucleation from centrosome, formation of bipolar spindles, chromosome congression, and chromosome segregation [18]. It is viral to ensure proper mitotic progression for normal cell division [19]. Cells alerts these processes with the spindle-assembly checkpoint (SAC) which is activated by misaligned chromosomes and

* Corresponding author. Fax: +82 2 710 9871.
E-mail address: cyjang@sookmyung.ac.kr (C.-Y. Jang).

http://dx.doi.org/10.1016/j.bbrc.2014.01.124
0006-291X/

abnormal spindle orientation and as a result arrests defective mitotic cells in metaphase [20]. The SAC monitors the capture of kinetochore by spindle MTs and the tension between inter-kinetochores by bi-oriented mitotic spindles. When spindle MTs capture all kinetochores and form bi-orientation, SAC is inactivated by releasing SAC proteins such as Mad2 and BubR1 from kinetochores and consents to initiate anaphase onset. In this regard, the SAC prevents mis-segregation of chromosomes and aneuploidy which can cause tumorigenesis.

Sirt3 has been identified as a cell division gene through time-lapse microscopy, because depletion of Sirt3 causes misaligned chromosomes and mitotic cell death [21]. This report prompted us to investigate the precise mitotic function of Sirt3 and its mechanism during mitosis. Depletion of Sirt3 caused unaligned chromosome which was not attached by spindle MTs and activated SAC to arrest cells in metaphase. Furthermore, depletion of Sirt3 increased the stability of spindle MTs, which, in turn, increased spindle polymerization. Thus, we can conclude that Sirt3 is a new mitotic regulator that controls chromosome alignment by regulating the stability of mitotic spindles in mitosis.

2. Materials and methods

2.1. Antibodies

The full-length Sirt3 gene was subcloned into the pCMV-Tag 5 vector with a C-terminal myc tag (Stratagene, USA). Sirt3H248Y mutant in pCDNA4-Myc-HisA vector was purchased from Addgene (UAS).

Anti-Sirt3 and anti-Tpx2 antibodies were purchased from GeneTex (USA). Rabbit antibodies against Mad2 and BubR1 were described previously [22]. Anti-Hsp90 antibody was purchased from Santa Cruz Biotechnology (USA). Anti-acetylated tubulin antibody was purchased from Sigma (USA). Anti-β-tubulin E7 monoclonal antibody was obtained from the Developmental Studies Hybridoma Bank (USA).

2.2. Cell culture and transfection

HeLa cells were cultured in Dulbecco's modified Eagle's medium (DMEM, WelGENE Inc.) supplemented with 10% fetal bovine serum (FBS, Invitrogen), penicillin (100 units/mL) and 100 μg/mL streptomycin (Invitrogen). The cells were maintained at 37 °C in a humidified atmosphere containing 5% CO_2. siRNAs were synthesized by Bioneer, Inc. (South Korea). The sequence targeting Sirt3 was 5′-GUCCAUAUCUUUUUCUGUGTT-3′. The control siRNA (siGL2) was 5′-CGTACGCGGAATACTTCGATT-3′. siRNAs were transfected into HeLa cells using DharmaFect 1 (Dharmacon, Inc.). DNA transfection was performed using Lipofectamine 2000 (Invitrogen, USA) as instructed by the manufacturer.

2.3. Immunofluorescence

HeLa cells on coverglasses were fixed with methanol at −20 °C for 30 min. Alternatively, cells were extracted with the BRB80-T buffer (80 mM PIPES, pH 6.8, 1 mM $MgCl_2$, 5 mM EGTA and 0.5% Triton X-100) and then fixed with 4% paraformaldehyde for 15 min at room temperature. The fixed cells were then permeabilized and blocked with PBS-BT (1 × PBS, 3% BSA, and 0.1% Triton X-100) for 30 min at room temperature. Coverslips were then incubated in primary and secondary antibodies diluted in PBS-BT. Images were acquired using an LSM image examiner (Carl Zeiss, Germany) under a Zeiss LSM510 confocal microscope and 63× oil immersion lens. Some images were acquired with AxioVision 4.8.2 (Carl Zeiss) under a Zeiss Axiovert 200 M microscope using a 1.4 NA plan-Apo 100× oil immersion lens and a HRm CCD camera. Deconvolved images were obtained using AutoDeblur v9.1 and AutoVisualizer v9.1 (AutoQuant Imaging).

2.4. Live cell image

For time-lapse microscopy, HeLa cells stably expressing GFP-H2B were cultured in Leibovitz's L-15 medium (Invitrogen) supplemented with 10% fetal bovine serum (Invitrogen) and 2 mM L-glutamine (Invitrogen). Cells were placed into a sealed growth chamber heated to 37 °C and observed on a Zeiss Axiovert 200 M microscope with a 20× lens. Images were acquired every three minutes for five hours with AxioVision 4.8.2 (Carl Zeiss).

For FLIP, HeLa cells stably expressing GFP-α-tubulin were transfected with a control or siSirt3 and placed in a sealed growth chamber heated to 37 °C. Cytoplasmic GFP-α-tubulin was photobleached with a laser and images were acquired at 0.632 s intervals for 337.459 s with ZEN (Carl Zeiss) under a LSM 700 confocal microscope (Carl Zeiss) with a 40× lens. 10 half-spindles from 10 metaphase cells in each transfection were analyzed by measuring the absolute GFP-α-tubulin fluorescence intensity in a defined circular area contained entirely within each half-spindle. Fluorescence intensities for each half-spindle were normalized to their maximum intensity at the beginning of the time lapse and the 10 normalized datasets were averaged to generate a single trace for each transfection.

2.5. Measurement of intracellular ROS levels

The 2′,7′-dichlorofluorescein diacetate (DCFH-DA) was used to monitor the intracellular ROS levels. After transfection with Sirt3 siRNA, cells were plated in 96 well plates at a density of 5×10^5 cells/well. DCFH-DA was added to transfected cells at a final concentration of 5 μM and cells were incubated for 30 min at 37 °C. Fluorescence intensity was measured using microplate reader at an excitation wavelength of 485 nm and an emission wavelength of 530 nm.

3. Results and discussion

3.1. Sirt3 controls mitotic progression

It has been suggested that Sirt3 may be a mitotic regulator due to the fact that its depletion induces mitotic cell death and metaphase alignment problems [21]. To investigate whether Sirt3 has mitotic functions, human HeLa cells were transfected with siRNA against Sirt3 (Fig. 1A and B). As shown in Fig. 1A, Sirt3 showed no subcellular localization on the mitotic structures such as mitotic spindle, the centrosome, midbody, the kinetochore. Consistent with previous reports, however, depletion of Sirt3 with siRNA not only generated unaligned chromosomes but altered the shape of spindles and the amount of spindles. Quantitative analysis of mitotic progression indicated that sirt3 depleted cells were arrested in metaphase (Fig. 1C). Among metaphase cells, more than 30% of the cells contained unaligned chromosomes (Fig. 1D), indicating that Sirt3 is involved in chromosome congression to the mitotic equator. Furthermore, removal of Sirt3 increased the density of spindles (Fig. 1E) and resulted in an abnormal spindle shape (Fig. 1B), suggesting that Sirt3 controls spindle formation and stability. Because reactive oxygen species (ROS) generated by depletion of mitochondrial Sirt3 could directly affect mitosis, we analyzed ROS level and mitotic defects in Sirt3 depleted cells with or without antioxidant, N-acetylcysteine (NAC). As expected, ROS caused by Sirt3 depletion was decreased with NAC treatment (Fig. 1F). However, una-

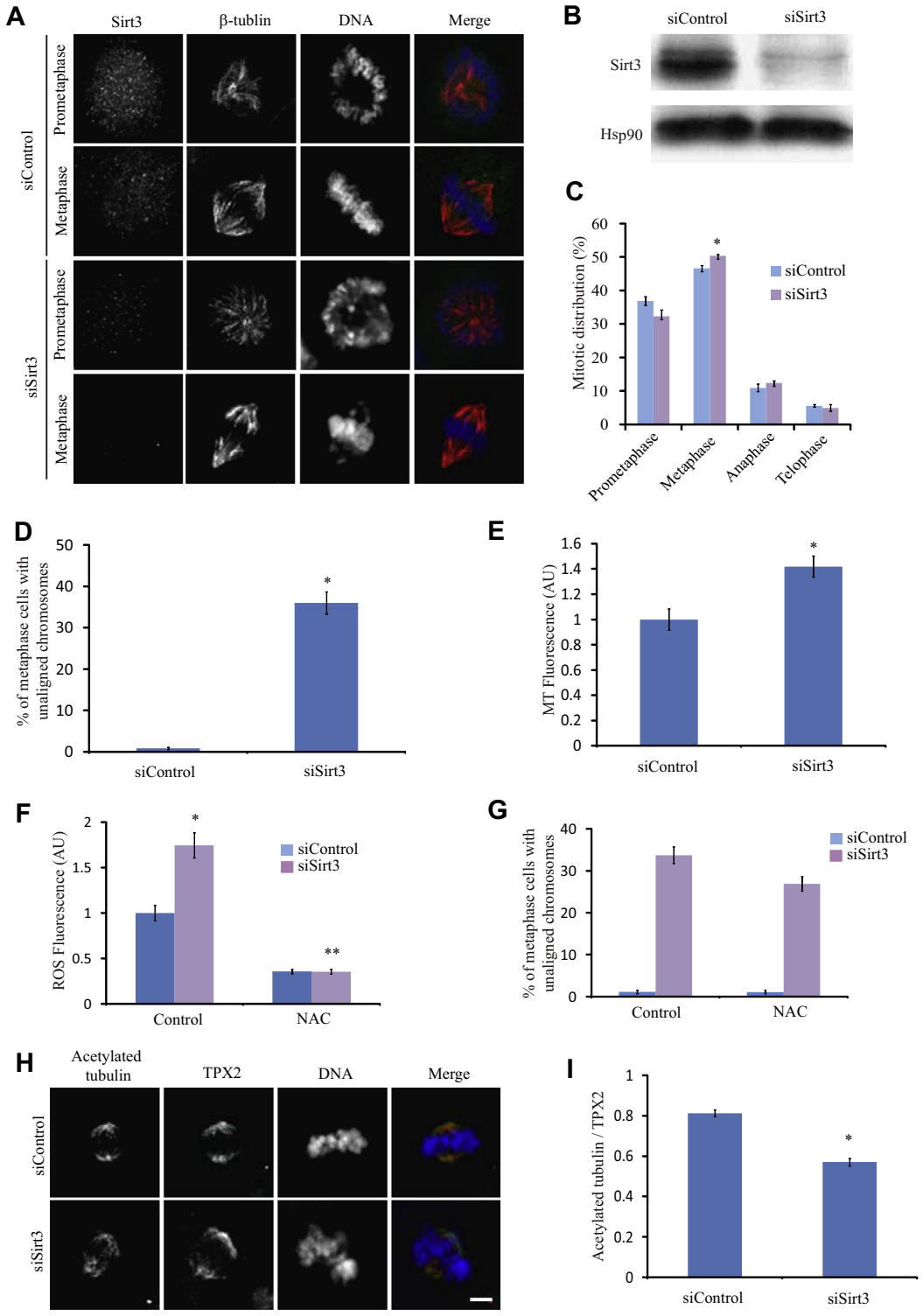

Fig. 1. Depletion of Sirt3 causes chromosome alignment defect. (A and B) HeLa cells were transfected with control (siControl) or Sirt3-specific siRNAs (siSirt3). Cells were fixed with MeOH at 72 h post-transfection and stained with antibodies as indicated. (A). Images are maximum projections from z stacks of representative cells stained for Sirt3 (green), β-tubulin (red), and DNA (blue). Scale bar, 5 μm. Also, the cells were harvested at 72 h post-transfection and lysates were analyzed by Western blotting against the indicated antibodies. (B) HSP90 served as a loading control. (C) The percentage of mitotic cells with the indicated phases were quantified and plotted ($n = 300$ cells for each quantification). $^{*}p < 0.005821$ (two-tailed t test relative to control cells). (D) The percentage of metaphase cells with unaligned chromosomes over total metaphase cells were quantified and plotted. $^{*}p < 2.39 \times 10^{-5}$ (two-tailed t test relative to control cells). (E) MT fluorescence intensity in metaphase cells was quantified and plotted ($n = 10$ cells). Images were acquired under a constant exposure time for the β-tubulin channel. Error bars, SEM. $^{*}p < 1.66 \times 10^{-9}$ (two-tailed t test relative to control cells). (F and G) ROS fluorescence intensity was measured from control or Sirt3 depleted cells with or without 10 mM NAC treatment (F). $^{*}p < 3.41268 \times 10^{-9}$ (two-tailed t test relative to control cells), $^{**}p < 1.03597 \times 10^{-13}$ (two-tailed t test relative to siSirt3 cells without NAC treatment). The percentage of metaphase cells with unaligned chromosomes over total metaphase cells were quantified and plotted (G). (H and I) HeLa cells were fixed with MeOH at 72 h post-transfection and stained with antibodies as indicated (H). Images are maximum projections from z stacks of representative cells stained for acetylated tubulin (green), TPX2 (red), and DNA (blue). Scale bar, 5 μm. The fluorescence intensity of acetylated tubulin over TPX2 as a spindle density was quantified and plotted (I). $^{*}p < 2.7 \times 10^{-8}$ (two-tailed t test relative to control cells). (For interpretation of the references to color in this figure legend, the reader is referred to the web version of this article.)

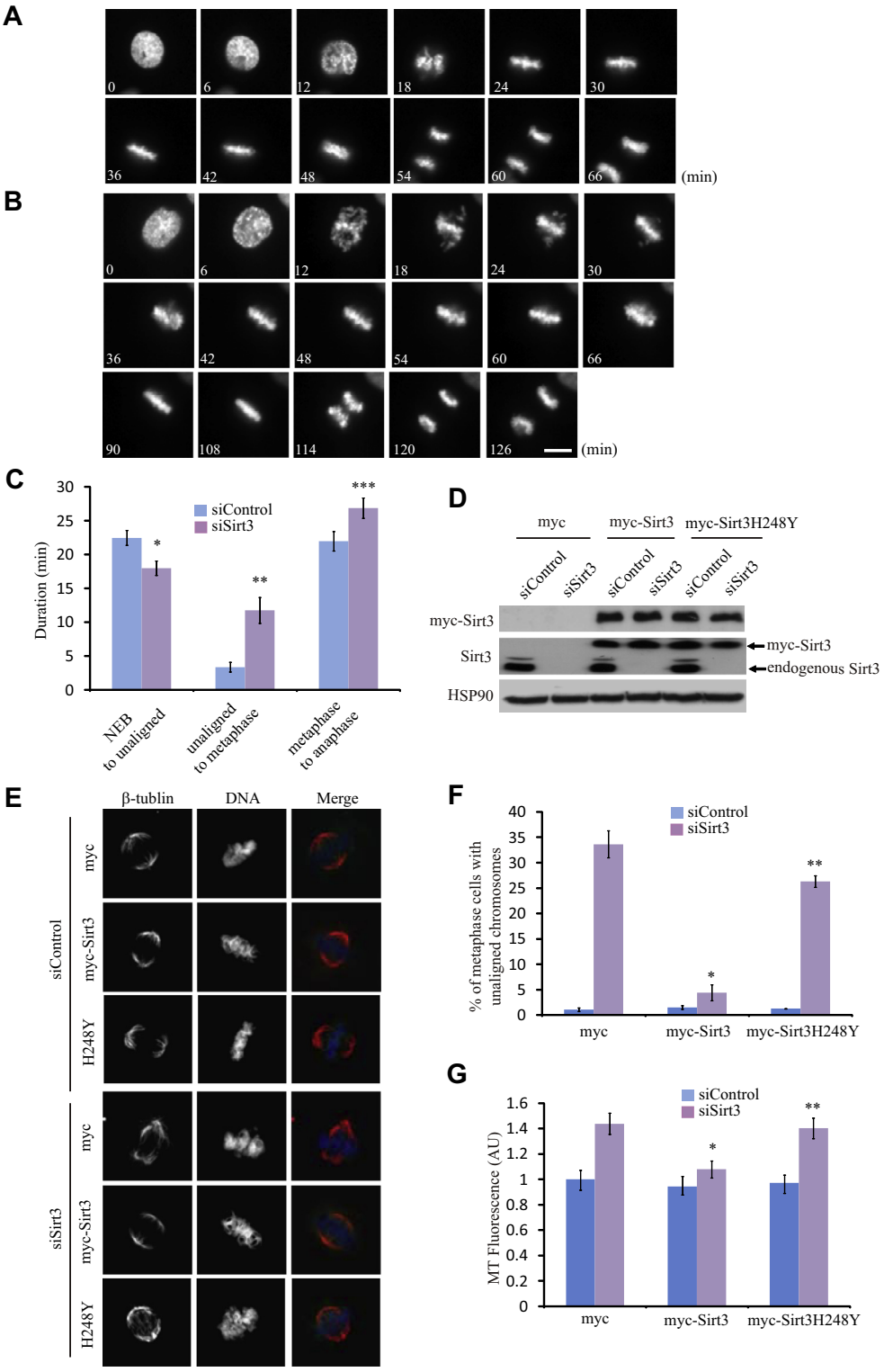

Fig. 2. Sirt3 is involved in mitotic progression. (A and B) HeLa/GFP-Histon H2B cells were transfected with control (A) or Sirt3-specific (B) siRNAs and imaged for GFP-H2B by time laps starting from 72 h after transfection. Images were captured every 3 min to monitor mitotic progression. Still frames from time-lapse movies of representative cells are shown. Scale bar, 10 μm. (C) The duration from nuclear envelope breakdown (NEB) to the formation of a bipolar spindle/metaphase plate with some unaligned chromosomes (NEB to unaligned), from the unaligned state to metaphase without unaligned chromosomes (unaligned to metaphase), and from metaphase without unaligned chromosomes to anaphase (metaphase to anaphase) were determined for control and Sirt3-depleted cells ($n = 50$ cells). $^{*}p < 4.39 \times 10^{-11}$; $^{**}p < 1.114 \times 10^{-17}$; $^{***}p < 2.475 \times 10^{-8}$ (two-tailed t-test relative to control cells). Error bars, SEM. (D–G) 48 h after siRNA transfection, HeLa cells were transfected with myc, myc-Sirt3 or myc-Sirt3H248Y and analyzed by Western blotting against the indicated antibodies. HSP90 serving as a loading control (D). Cells were fixed ad stained for indicated antigens and images of myc-positive cells were acquired under a constant exposure in each channel for all cells. Scale bar, 5 μm (E). The percentage of metaphase cells with unaligned chromosomes over total metaphase cells in myc-positive cells were quantified and plotted ($n = 100$ cells from three independent experiments). Error bars, SEM. $^{*}p < 6.28125 \times 10^{-5}$ (two-tailed t-test relative to Sirt3 depleted and myc transfected cells), $^{**}p < 3.88 \times 10^{-5}$ (two-tailed t-test relative to Sirt3 depleted and myc-Sirt3 transfected cells) (F). Total immunofluorescence intensity for β-tubulin ($n = 10$ cells for each quantification) was quantified and plotted. $^{*}p < 3.7355 \times 10^{-9}$ (two-tailed t-test relative to Sirt3 depleted and myc transfected cells), $^{**}p < 1.38797 \times 10^{-8}$ (two-tailed t-test relative to Sirt3 depleted and myc-Sirt3 transfected cells) (G).

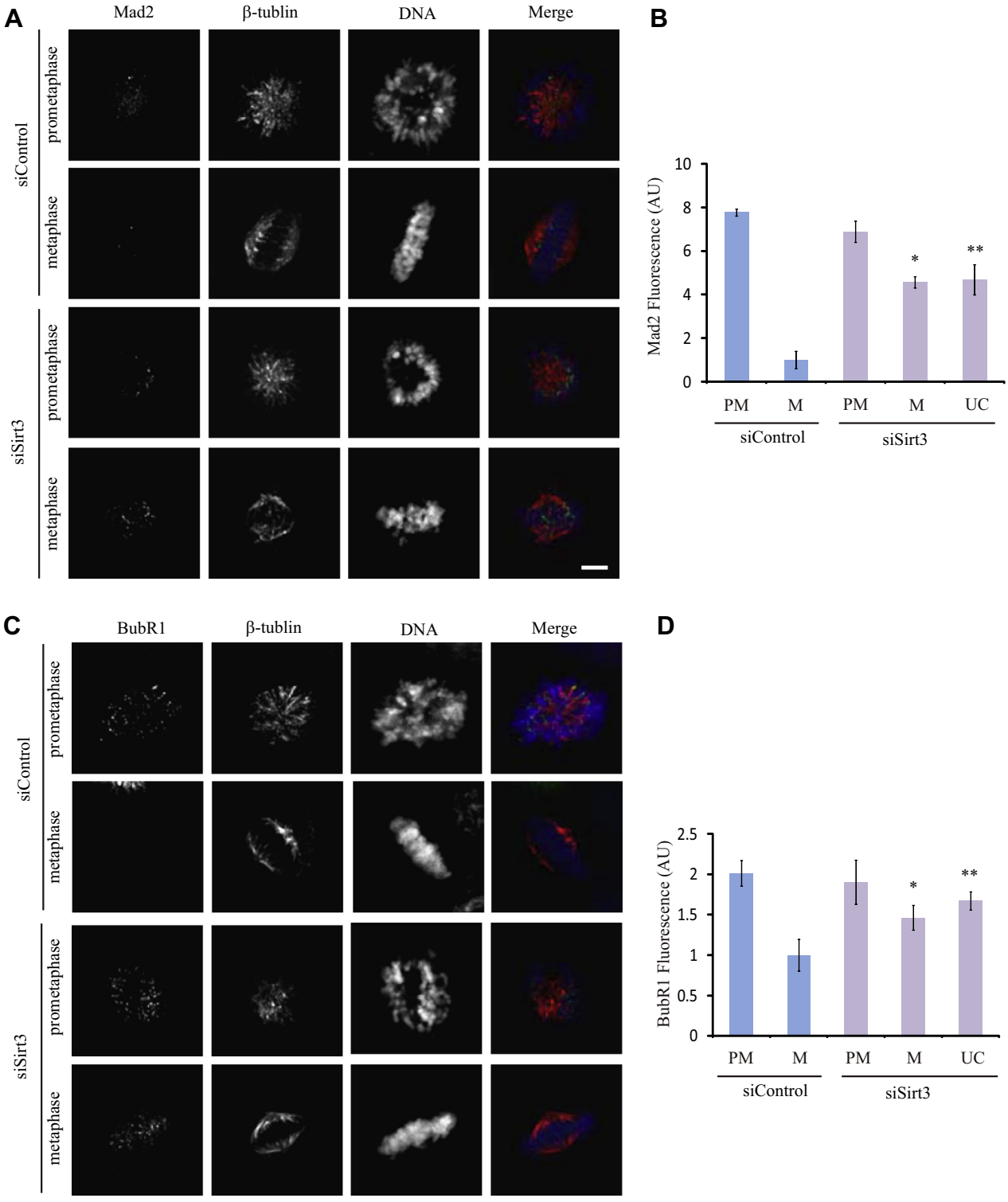

Fig. 3. Depletion of Sirt3 activates SAC. HeLa cells were transfected with control (siControl) or Sirt3-specific siRNAs. Cells were fixed at 72 h post-transfection and stained with the indicated antibodies. (A) Shown are maximum projections from z stacks of representative control or Sirt3-depleted cells stained for Mad2 (green), β-tubulin (red), and DNA (blue). Scale bar, 5 μm. (B) Mad2 signals on kinetochores were quantified in five control of Sirt3-depleted cells in (A) at prometaphase (PM), metaphase (M), and unaligned chromosomes (UN; $n > 50$ kinetochores for each quantification). Error bars show SEM. $^{*}p < 1.73 \times 10^{-93}$; $^{**}p < 4.9 \times 10^{-59}$ (two tailed t-test relative to control metaphase cells). (C) Shown are maximum projections from z stacks of representative control or Sirt3-depleted cells stained for BubR1 (green), β-tubulin (red), and DNA (blue). Scale bar, 5 μm. (D) BubR1 signals on kinetochores in (C) were quantified in five control of Sirt3-depleted cells at prometaphase (PM), metaphase (M), and unaligned chromosomes (UN; $n > 50$ kinetochores for each quantification). Error bars show SEM. $^{*}p < 3.6 \times 10^{-27}$; $^{**}p < 7.4 \times 10^{-44}$ (two tailed t-test relative to control metaphase cells). (For interpretation of the references to color in this figure legend, the reader is referred to the web version of this article.)

ligned chromosome generated by Sirt3 depletion was not rescued completely with NAC treatment (Fig. 1G), indicating that Sirt3 itself is involved in mitotic processes. To determine whether Sirt3 acts as tubulin deacetylase like Sirt2, we next analyzed the level of acetylated tubulin in Sirt3 depleted cells. Sirt3 depleted cells showed no significant levels of acetylated tubulin (Fig. 1H and I), suggesting that Sirt3 may not be a deacetylase of tubulin unlike Sirt2.

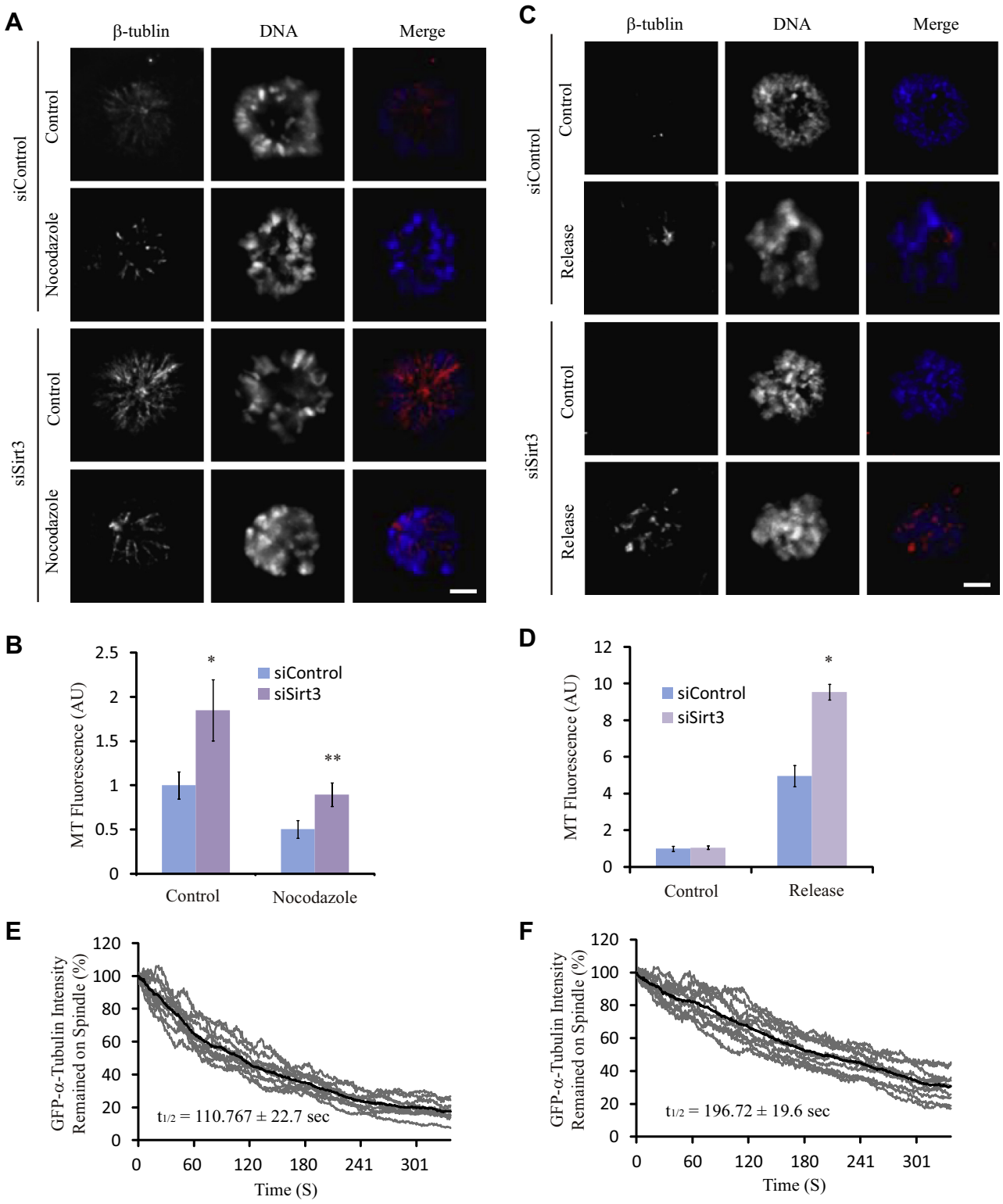

Fig. 4. Sirt3 regulates spindle microtubule stabilization. (A) HeLa cells were transfected with a siControl or siSirt3. Control or rpS3-depleted cells were treated with 1 μg/mL nocodazole for 3 min and analyzed by immunofluorescence staining of β-tubulin. Scale bar, 5 μm. (B) Images for β-tubulin in (A) were acquired under a constant exposure time. β-Tubulin immunofluorescence intensity on spindles was quantified and normalized to control sample ($n = 10$ cells for each quantification). $^{*}p < 0.001025$; $^{**}p < 0.000769$ (two-tailed t test relative to control cells). Error bars, SEM. (C) HeLa cells were transfected with a siControl or siSirt3. Control or rpS3-depleted cells were treated with 1 μg/mL nocodazole for 10 min at 37 °C, washed, released into fresh media, and fixed with MeOH at the 3 min timepoints. Cells were analyzed by immunofluorescence staining of β-tubulin. Scale bar, 5 μm. (D) Images for β-tubulin in (C) were acquired under a constant exposure time. β-Tubulin immunofluorescence intensity on spindles was quantified and normalized to control sample ($n = 10$ cells for each quantification). $^{*}p < 9.17535 \times 10^{-14}$ (two-tailed t test relative to control cells). Error bars, SEM. (E and F) HeLa cells stably expressing GFP-α-tubulin were transfected with control (E) or Sirt3-specific (F) siRNAs. GFP fluorescence intensity was acquired every 0.632 s while a photobleaching laser was focused to a diffraction-limited spot in the cytoplasm away from the spindle. 10 half-spindles from 10 metaphase cells were quantified and fluorescence signals for each half spindle were normalized to their intensity at 0 s and averaged across the 10 half-spindles at each time point (thick traces). Turnover half-lives for GFP-α-tubulin on the spindle were calculated from the averaged fluorescence signal traces. $p < 1.32894 \times 10^{-30}$ (two-tailed t-test relative to control cells).

To further ascertain the mitotic function of Sirt3, the intercellular function of Sirt3 was analyzed by time-laps imaging of HeLa cells that stably express GFP-Histone H2B. As shown in Fig. 2A and B, depletion of Sirt3 caused unaligned chromosomes in metaphase. Quantitative analysis of mitotic duration indicated that depletion of Sirt3 significantly prolonged the duration of metaphase with unaligned chromosomes (from the unaligned state to metaphase without unaligned chromosomes) (Fig. 2C). Also, the duration of metaphase (from the initial formation of the metaphase plate to the onset of anaphase) was significantly increased (Fig. 2B and C), indicating that unaligned chromosomes generated by Sirt3 depletion arrest cells in metaphase.

To confirm whether mitotic defects in Sirt3-depleted cells result from the absence of Sirt3, we performed rescue experiment. After depletion of Sirt3, HeLa cells were transfected with myc-Sirt3 to re-express exogenous myc-Sirt3 (Fig. 2D). Notably, expression of the myc-Sirt3 in cells depleted for endogenous Sirt3 successfully restored chromosome alignment (Fig. 2E and F) and spindle formation (Fig. 2E and G). However, Sirt3H248Y inactive mutant did not rescue mitotic defects caused by Sirt3 depletion (Fig. 2F and G), suggesting that the deacetylase activity of Sirt3 is involved in mitotic processes. Overall, these data indicate that Sirt3 is required for proper mitotic progression such as chromosome alignment and spindle formation.

3.2. Depletion of Sirt3 activates the spindle assembly checkpoint

The SAC prevents the initiation of anaphase when cells are detected to have chromosome alignment in metaphase by the process of inhibiting cell division cycle 20 (CDC20), a receptor protein of the ubiquitin ligase anaphase-promoting complex/cyclosome (APC/C) [19]. The APC/C^{CDC20} targets cyclin B and securin to destroy by the 26S proteasome. Securin is an inhibitor of separase, which, in turn, degrades the cohesin complex. Sister chromatids are held together by the cohesin complex before the onset of anaphase. When all chromosomes are captured by mitotic spindles and become bi-orientated between two spindle poles, inactivation of SAC relieves mitotic arrest and approves this chain of events, resulting in anaphase onset.

Next, we investigated the reason why unaligned chromosomes were generated in Sirt3 depleted cells. To determine whether the problem of congression of mitotic chromosomes is caused by a lack of MT attachment, we analyzed the amount of Mad2, which is released from kinetochores after MT attachment. As expected, Mad2 was present on the kinetochores of control and Sirt3 knockdown cells in prometaphase and disappeared in metaphase in control cells. However, it did not disappear from the kinetochores of both aligned and unaligned chromosomes in metaphase in Sirt3 knockdown cells (Fig. 3A and B), indicating that MTs are not attached to kinetochores in the absence of Sirt3. We next analyzed the amount of BubR1, which is disappeared from kinetochores after generating tension across sister kinetochores by bi-oriented spindles. Whereas BubR1 was released from kinetochores of control cells at metaphase, it was not released from the kinetochores of Sirt3 knockdown cells in metaphase (Fig. 3C and D) due to the lack of MT attachment. Thus, Sirt3 is required for spindle attachment at kinetochores and chromosome congression to the metaphase plate.

3.3. Sirt3 controls spindle dynamics

The driving force of chromosome movement, such as congression to the metaphase plate and segregation in anaphase, is spindle dynamics [18]. Base on the search and capture model, spindle attachment to kinetochores also depends on spindle dynamics. Therefore, a decrease in spindle dynamics by increasing spindle MT stability can result in defects during spindle attachment. MT density was increased in Sirt3 depleted cells compared with that in control cells (Fig. 1B and E). To confirm whether spindle dynamics is decreased in Sirt3 knockdown cells, we analyzed MT-depolymerization in the presence of nocodazole. As shown in Fig. 4A and B, the MT density was higher in Sirt3 depleted cells under conditions that destabilized MTs with nocodazole. We next determined the kinetics of MT polymerization after completely depolymerizing spindle MTs with nocodazole treatment. Repolymerization of MTs was faster in Sirt3 depleted cells than in control cells (Fig. 4C and D), suggesting that Sirt3 destabilizes mitotic spindles and increases spindle dynamics. To further confirm whether Sirt3 regulates spindle dynamics, we measured the turnover rate of α/β-tubulin heterodimers on the mitotic spindle through a fluorescence loss in photobleaching (FLIP) experiment. As expected, the half-life of GFP-α-tubulin on the metaphase spindle in siSirt3 cells was increased (Fig. 4E and F), suggesting that Sirt3 increases the rate of MT turnover on metaphase spindles to generate the tension across sister kinetochores for chromosome movement.

The function of mitotic spindles is to capture chromosomes for alignment at the metaphase plate and to segregate two sister chromatids toward the spindle pole [18]. Chromosome movement is powered by kinetochore-mediated depolymerization of MT plus ends. Spindle dynamics is regulated by microtubule associated proteins (MAPs) such as EB1, HURP, and DDA3 and by post-translational modifications of tubulin including tyrosination, phosphorylation, polyglutamylation, polyglycylation, and acetylation [23,24]. α-Tubulin is acetylated at lysine 40 which is found in stable MTs. During mitosis, spindle MTs are highly modified by polyglutamination, acetylation, and detyrosination, whereas astral MTs are mostly unmodified [25,26]. Even-though the acetylation enzyme has not been identified, HDAC6 and Sirt2 have been reported as a deacetylase for α-tubulin [27,28]. Sirt3 may not be a tubulin deacetylase, because depletion of Sirt3 was found not to increase acetylated tubulin, dramatically (Fig. 1F and G). However, Sirt3 depletion increased the amount of mitotic spindles (Fig. 1E), the spindle stability and polymerization (Fig. 4A and C), and decreased spindle dynamics (Fig. 4F). Therefore, it remains to be elucidated which mitotic regulators are direct substrates of Sirt3 to control spindle dynamics during mitosis.

In summary, we demonstrated that Sirt3 is required for spindle attachment to kinetochores and subsequent chromosome congression at the metaphase plate. Furthermore, Sirt3 functions as a mitotic deacetylase to control spindle dynamics by destabilizing spindle MTs. Our data clearly showed that Sirt3 is associated with chromosomal stability during mitosis.

Acknowledgment

This work was supported by the Sookmyung Women's University Research Grants (1-1103-0473).

References

[1] B.J. North, E. Verdin, Sirtuins: Sir2-related NAD-dependent protein deacetylases, Genome Biol. 5 (2004) 224.
[2] D. Chen, L. Guarente, SIR2: a potential target for calorie restriction mimetics, Trends Mol. Med. 13 (2007) 64–71.
[3] J.C. Milne, J.M. Denu, The Sirtuin family: therapeutic targets to treat diseases of aging, Curr. Opin. Chem. Biol. 12 (2008) 11–17.
[4] M.C. Haigis, D.A. Sinclair, Mammalian sirtuins: biological insights and disease relevance, Annu. Rev. Pathol. 5 (2010) 253–295.
[5] S. Michan, D. Sinclair, Sirtuins in mammals: insights into their biological function, Biochem. J. 404 (2007) 1–13.
[6] A. Vaquero, R. Sternglanz, D. Reinberg, NAD+-dependent deacetylation of H4 lysine 16 by class III HDACs, Oncogene 26 (2007) 5505–5520.
[7] M.C. Haigis, L.P. Guarente, Mammalian sirtuins–emerging roles in physiology, aging, and calorie restriction, Genes Dev. 20 (2006) 2913–2921.
[8] T. Inoue, M. Hiratsuka, M. Osaki, H. Yamada, I. Kishimoto, S. Yamaguchi, S. Nakano, M. Katoh, H. Ito, M. Oshimura, SIRT2, a tubulin deacetylase, acts to

block the entry to chromosome condensation in response to mitotic stress, Oncogene 26 (2007) 945–957.
[9] A. Giralt, F. Villarroya, SIRT3, a pivotal actor in mitochondrial functions: metabolism, cell death and aging, Biochem. J. 444 (2012) 1–10.
[10] M.C. Haigis, R. Mostoslavsky, K.M. Haigis, K. Fahie, D.C. Christodoulou, A.J. Murphy, D.M. Valenzuela, G.D. Yancopoulos, M. Karow, G. Blander, C. Wolberger, T.A. Prolla, R. Weindruch, F.W. Alt, L. Guarente, SIRT4 inhibits glutamate dehydrogenase and opposes the effects of calorie restriction in pancreatic beta cells, Cell 126 (2006) 941–954.
[11] P.J. Fernandez-Marcos, M. Serrano, Sirt4: the glutamine gatekeeper, Cancer Cell 23 (2013) 427–428.
[12] T. Nakagawa, L. Guarente, Urea cycle regulation by mitochondrial sirtuin, SIRT5, Aging (Albany NY) 1 (2009) 578–581.
[13] J. Du, Y. Zhou, X. Su, J.J. Yu, S. Khan, H. Jiang, J. Kim, J. Woo, J.H. Kim, B.H. Choi, B. He, W. Chen, S. Zhang, R.A. Cerione, J. Auwerx, Q. Hao, H. Lin, Sirt5 is a NAD-dependent protein lysine demalonylase and desuccinylase, Science 334 (2011) 806–809.
[14] C. Sebastian, B.M. Zwaans, D.M. Silberman, M. Gymrek, A. Goren, L. Zhong, O. Ram, J. Truelove, A.R. Guimaraes, D. Toiber, C. Cosentino, J.K. Greenson, A.I. MacDonald, L. McGlynn, F. Maxwell, J. Edwards, S. Giacosa, E. Guccione, R. Weissleder, B.E. Bernstein, A. Regev, P.G. Shiels, D.B. Lombard, R. Mostoslavsky, The histone deacetylase SIRT6 is a tumor suppressor that controls cancer metabolism, Cell 151 (2012) 1185–1199.
[15] E. Ford, R. Voit, G. Liszt, C. Magin, I. Grummt, L. Guarente, Mammalian Sir2 homolog SIRT7 is an activator of RNA polymerase I transcription, Genes Dev. 20 (2006) 1075–1080.
[16] R.H. Wang, K. Sengupta, C. Li, H.S. Kim, L. Cao, C. Xiao, S. Kim, X. Xu, Y. Zheng, B. Chilton, R. Jia, Z.M. Zheng, E. Appella, X.W. Wang, T. Ried, C.X. Deng, Impaired DNA damage response, genome instability, and tumorigenesis in SIRT1 mutant mice, Cancer Cell 14 (2008) 312–323.
[17] B.J. North, E. Verdin, Interphase nucleo-cytoplasmic shuttling and localization of SIRT2 during mitosis, PLoS One 2 (2007) e784.
[18] S.L. Kline-Smith, C.E. Walczak, Mitotic spindle assembly and chromosome segregation: refocusing on microtubule dynamics, Mol. Cell 15 (2004) 317–327.
[19] K.I. Nakayama, K. Nakayama, Ubiquitin ligases: cell-cycle control and cancer, Nat. Rev. Cancer 6 (2006) 369–381.
[20] A. Musacchio, E.D. Salmon, The spindle-assembly checkpoint in space and time, Nat. Rev. Mol. Cell Biol. 8 (2007) 379–393.
[21] B. Neumann, T. Walter, J.K. Heriche, J. Bulkescher, H. Erfle, C. Conrad, P. Rogers, I. Poser, M. Held, U. Liebel, C. Cetin, F. Sieckmann, G. Pau, R. Kabbe, A. Wunsche, V. Satagopam, M.H. Schmitz, C. Chapuis, D.W. Gerlich, R. Schneider, R. Eils, W. Huber, J.M. Peters, A.A. Hyman, R. Durbin, R. Pepperkok, J. Ellenberg, Phenotypic profiling of the human genome by time-lapse microscopy reveals cell division genes, Nature 464 (2010) 721–727.
[22] J. Wong, G. Fang, HURP controls spindle dynamics to promote proper interkinetochore tension and efficient kinetochore capture, J. Cell Biol. 173 (2006) 879–891.
[23] C.Y. Jang, J. Wong, J.A. Coppinger, A. Seki, J.R. Yates 3rd, G. Fang, DDA3 recruits microtubule depolymerase Kif2a to spindle poles and controls spindle dynamics and mitotic chromosome movement, J. Cell Biol. 181 (2008) 255–267.
[24] J.W. Hammond, D. Cai, K.J. Verhey, Tubulin modifications and their cellular functions, Curr. Opin. Cell Biol. 20 (2008) 71–76.
[25] K.J. Verhey, J. Gaertig, The tubulin code, Cell Cycle 6 (2007) 2152–2160.
[26] S. Westermann, K. Weber, Post-translational modifications regulate microtubule function, Nat. Rev. Mol. Cell Biol. 4 (2003) 938–947.
[27] C. Hubbert, A. Guardiola, R. Shao, Y. Kawaguchi, A. Ito, A. Nixon, M. Yoshida, X.F. Wang, T.P. Yao, HDAC6 is a microtubule-associated deacetylase, Nature 417 (2002) 455–458.
[28] B.J. North, B.L. Marshall, M.T. Borra, J.M. Denu, E. Verdin, The human Sir2 ortholog, SIRT2, is an NAD+-dependent tubulin deacetylase, Mol. Cell 11 (2003) 437–444.